

Stratospheric ozone changes from explosive tropical volcanoes: Modelling and ice core constraints

Alison Ming^{1,1}, V Holly L Winton^{2,2}, James Keeble^{1,1}, Nathan Luke Abraham^{3,3}, Mohit Dalvi^{4,4}, Paul Thomas Griffiths^{1,1}, Nicolas Caillon^{5,5}, Anna E Jones^{2,2}, Robert Mulvaney^{2,2}, Markus Michael Frey^{2,2}, Xin Yang^{1,1}, and Joel Savarino⁶

¹University of Cambridge

²British Antarctic Survey

³NCAS, University of Cambridge

⁴Met Office

⁵Lab. des Sciences du Climat et de l'Environnement

⁶CNRS en Alpes

November 30, 2022

Abstract

Major tropical volcanic eruptions have emitted large quantities of stratospheric sulphate and are potential sources of stratospheric chlorine although this is less well constrained by observations. This study combines model and ice core analysis to investigate past changes in total column ozone. Historic eruptions are a good analogue for future eruptions as stratospheric chlorine levels have been decreasing since the year 2000. We perturb the pre-industrial atmosphere of a chemistry-climate model with high and low emissions of sulphate and chlorine. The sign of the resulting Antarctic ozone change is highly sensitive to the background stratospheric chlorine loading. In the first year, the response is dynamical, with ozone increases over Antarctica. In the high HCl (10 Tg emission) experiment, the injected chlorine is slowly transported to the polar regions with subsequent chemical ozone depletion. These model results are then compared to measurements of the stable nitrogen isotopic ratio, $\delta^{15}\text{N}(\text{NO}-3)$, from a low snow accumulation Antarctic ice core from Dronning Maud Land (recovered in 2016-17). We expect ozone depletion to lead to increased surface ultraviolet (UV) radiation, enhanced air-snow nitrate photo-chemistry and enrichment in $\delta^{15}\text{N}(\text{NO}-3)$ in the ice core. We focus on the possible ozone depletion event that followed the largest volcanic eruption in the past 1000 years, Samalas in 1257. The characteristic sulphate signal from this volcano is present in the ice-core but the variability in the $\delta^{15}\text{N}(\text{NO}-3)$ dominates any signal arising from changes in UV from ozone depletion. Whether Samalas caused ozone depletion over Antarctica remains an open question.

Stratospheric ozone changes from explosive tropical volcanoes: Modelling and ice core constraints

Alison Ming^{1,2}, V. Holly L. Winton¹, James Keeble^{2,3}, Nathan L. Abraham^{2,3},
Mohit C. Dalvi⁴, Paul Griffiths^{2,3}, Nicolas Caillon⁵, Anna E. Jones¹, Robert
Mulvaney¹, Markus M. Frey¹, Xin Yang¹

¹British Antarctic Survey

²University of Cambridge, U.K.

³National Centre for Atmospheric Science, U.K.

⁴Met Office Hadley Centre, Exeter, UK, EX1 3XB

⁵Institut des Géosciences de l'Environnement, CNRS, France

Key Points:

- The tropical volcanic eruption in the model shows that the sign of the ozone change is highly sensitive to stratospheric chlorine amounts.
- $\delta^{15}\text{N}(\text{NO}_3^-)$ (a proxy for surface ultra-violet radiation) from the Samalas eruption is obscured by inter-annual variability in the ice core.
- $\delta^{15}\text{N}(\text{NO}_3^-)$ changes are unlikely to be synchronous with volcanic sulphate peaks due to different pathways for these signals to reach the ice.

Corresponding author: Alison Ming, A.Ming@damtp.cam.ac.uk

Abstract

Major tropical volcanic eruptions have emitted large quantities of stratospheric sulphate and are potential sources of stratospheric chlorine although this is less well constrained by observations. This study combines model and ice core analysis to investigate past changes in total column ozone. Historic eruptions are a good analogue for future eruptions as stratospheric chlorine levels have been decreasing since the year 2000. We perturb the pre-industrial atmosphere of a chemistry-climate model with high and low emissions of sulphate and chlorine. The sign of the resulting Antarctic ozone change is highly sensitive to the background stratospheric chlorine loading. In the first year, the response is dynamical, with ozone increases over Antarctica. In the high HCl (10 Tg emission) experiment, the injected chlorine is slowly transported to the polar regions with subsequent chemical ozone depletion. These model results are then compared to measurements of the stable nitrogen isotopic ratio, $\delta^{15}\text{N}(\text{NO}_3^-)$, from a low snow accumulation Antarctic ice core from Dronning Maud Land (recovered in 2016-17). We expect ozone depletion to lead to increased surface ultraviolet (UV) radiation, enhanced air-snow nitrate photo-chemistry and enrichment in $\delta^{15}\text{N}(\text{NO}_3^-)$ in the ice core. We focus on the possible ozone depletion event that followed the largest volcanic eruption in the past 1000 years, Samalas in 1257. The characteristic sulphate signal from this volcano is present in the ice-core but the variability in the $\delta^{15}\text{N}(\text{NO}_3^-)$ dominates any signal arising from changes in UV from ozone depletion. Whether Samalas caused ozone depletion over Antarctica remains an open question.

Plain Language Summary

Chlorine in the stratosphere destroys ozone that protects the Earth from harmful ultraviolet radiation. Volcanic eruptions in the tropics can emit sulphate and chlorine into the stratosphere. Chlorine levels are currently decreasing and to understand the impact of a volcanic eruption on stratospheric ozone in a future climate, historical eruptions are a useful analogue since the pre-industrial climate also had low chlorine levels. Using a chemistry climate model, we run a set of experiments where we inject different amounts of sulphate and chlorine into the stratosphere over the tropics to simulate different types and strengths of explosive volcanoes and we find that the ozone over Antarctica initially increases over the first year following the eruption. If the volcano emits a large amount of chlorine, ozone then decreases over Antarctica in years two to four following the eruption. We also compare our results to ice-core data around a large historic volcanic eruption, Samalas (1257).

1 Introduction

The ozone layer protects life on Earth from ultraviolet (UV) radiation. Explosive tropical volcanic eruptions can inject volcanic gases into the stratosphere which can disrupt the complex stratospheric chemistry and lead to substantial changes in total column ozone (Solomon, 1999; Robock & Oppenheimer, 2003, for a comprehensive review). Over the last 1000 years, a number of explosive tropical volcanoes have injected copious volumes of sulphur dioxide (SO_2) and hydrochloric acid (HCl) into the stratosphere. In the current atmosphere, a large sulphur dioxide injection is expected to cause polar ozone loss via heterogeneous chemical reactions because of high stratospheric chlorine levels from anthropogenic activities (Tie & Brasseur, 1995). In contrast, in a low chlorine environment, such as a pre-industrial atmosphere or a future atmosphere where the chlorine loading of the stratosphere has declined, it is widely accepted that an injection of sulphate from an explosive tropical volcanic eruption will lead to ozone gain over polar regions (Langematz et al., 2018, and references therein). To understand the future atmospheric impact of volcanic eruptions, studying historic eruptions is a useful analog.

67 Estimates of the amount of sulphur dioxide emitted into the stratosphere from eruptions
68 over the past 1000 years are highly variable. For example, sulfate mass concentration
69 records from ice core data give the following estimates for recent tropical eruptions:
70 ~ 10 to 20 Tg SO_2 from Mount Pinatubo in 1991 (Timmreck et al., 2018), ~ 60 Tg SO_2
71 from Mount Tambora in 1815 (Zanchettin et al., 2016) and ~ 100 to 140 Tg SO_2 from
72 the Samalás 1257 series of eruptions (Toohey & Sigl, 2017). Samalás is the largest eruption
73 over the last 1000 years and part of a series of 4 large eruptions over about 26 years.

74 Some types of explosive volcanoes also emit chlorine and other halogen compounds.
75 Volcanic stratospheric chlorine emissions are important for ozone destruction reactions
76 (Kutterolf et al., 2013) but are less well constrained, since the highly soluble HCl is scavenged
77 by processes in the volcanic plume (Halmer et al., 2002). In the stratosphere, HCl
78 is the dominant chlorine reservoir species and a source of reactive halogen such as chlorine
79 monoxide, ClO, that destroys ozone. A sophisticated plume model (Textor et al.,
80 2003) suggest that 10% to 20% of the HCl emitted would enter the stratosphere and recent
81 satellite observations have detected HCl injection into the stratosphere from explosive
82 volcanoes (Theys et al., 2014). Geo-chemical evidence by Vidal et al. (2016) suggests
83 that the Samalás eruption (1257, 8.4° S, 116.5° E) could have injected as much as
84 ~ 230 Tg HCl into the atmosphere. In contrast, observations during the 1991 Pinatubo
85 eruption show that the efficiency of the scavenging is highly dependent on atmospheric
86 conditions with barely detectable increases in stratospheric HCl following the eruption
87 (Wallace & Livingston, 1992). Volcanic HCl emissions and the fraction of HCl mass entering
88 the stratosphere are hence highly variable as these depend on the geochemistry of the eruption
89 and the efficiency of the scavenging processes respectively. The type and location of the eruption
90 also play a role.

91 The impact of an explosive eruption on stratospheric ozone also depends on dynamical
92 processes. Variability arising from the El Niño-Southern Oscillation (ENSO), the quasi-biennial
93 oscillation (QBO) and the variability in the Brewer-Dobson circulation are able to affect the
94 ozone response following the eruption (Lehner et al., 2016; Telford et al., 2009). In addition,
95 the radiative heating from the aerosol injection and associated changes to the planetary wave
96 flux from the troposphere are able to alter the stratospheric circulation and hence the transport
97 of aerosols and trace gases (Poberaj et al., 2011). Since the precise time of the year of the
98 historic eruption is often not known, these factors have to be taken into account in the model
99 simulations (Stevenson et al., 2017).

100 Ground-based observations of total column ozone (TCO) commenced in the 1920s
101 and captured the severe decline in the ozone layer resulting from anthropogenic production
102 of long-lived ozone destroying-halocarbons e.g., Harris et al. (2015, and references therein).
103 However, beyond the relatively short instrumental period, records of total column ozone are
104 non-existent and thus paleo-reconstructions are required to understand how natural phenomena,
105 such as volcanic eruptions, can impact the variability of total column ozone.
106

107 Recent research has focused on novel Antarctic ice core proxies of surface UV radiation,
108 which can provide constraints on past ozone variability as changes in total column ozone affect
109 the surface UV over Antarctica. The UV proxy is based on the stable isotopic composition of
110 nitrate ($\delta^{15}\text{N}(\text{NO}_3^-)$) at low accumulation sites in Antarctica (Frey et al., 2009). Theory,
111 laboratory and field experiments have shown that nitrate (NO_3^-) loss from snow and associated
112 isotopic enrichment of $\delta^{15}\text{N}(\text{NO}_3^-)$ in the NO_3^- fraction remaining in the snow is driven by
113 UV photolysis (Shi et al., 2019; Berhanu et al., 2014, 2015; Frey et al., 2009). Photolytically-
114 induced fractionation of the $\delta^{15}\text{N}(\text{NO}_3^-)$ signal eventually archived in firn and ice depends
115 on a number of site-specific factors aside from the UV irradiance including the snow physical
116 properties and the amount and timing of snow accumulation (Erbland et al., 2015, 2013;
117 Noro et al., 2018; Shi et al., 2018). The largest enrichment of $\delta^{15}\text{N}(\text{NO}_3^-)$ is observed at
118 low accumulation sites on the East

119 Antarctic Plateau, where near surface snow is exposed for more than one summer sea-
 120 son to incoming UV radiation (Erbland et al., 2013; Shi et al., 2018).

121 Winton et al. (2019) carried out a comprehensive field and modelling study of the
 122 air-snow transfer of NO_3^- at the low snowfall accumulation site at Kohnen Station in
 123 Dronning Maud Land (DML), East Antarctica as part of the ISOL-ICE (ISotopic con-
 124 straints of past Ozone Layer in polar ICE) project. At the DML site, NO_3^- is recycled
 125 three times before it is archived in the snowpack below a depth of 15 cm and within 0.75 years.
 126 Sensitivity analysis with a 1D air-snow model, TRANSITS (TRansfer of Atmospheric
 127 Nitrate Stable Isotopes To the Snow) (Erbland et al., 2015), of $\delta^{15}\text{N}(\text{NO}_3^-)$ at DML showed
 128 that the dominant factors controlling the archived $\delta^{15}\text{N}(\text{NO}_3^-)$ signature are the snow
 129 accumulation rate and e-folding depth of the surface snowpack for incident UV, with a
 130 smaller role from changes in the snowfall timing and TCO. The Winton et al. (2019) study
 131 sets the framework for the interpretation of a $\delta^{15}\text{N}(\text{NO}_3^-)$ record from the new ISOL-
 132 ICE ice core drilled in January 2017 at Kohnen Station in Dronning Maud Land, hence-
 133 forth referred to as the DML site following the terminology in Winton et al. (2019). The
 134 DML region experiences low annual accumulation rates ($< 100 \text{ g cm}^{-2} \text{ yr}^{-1}$) but ice cores
 135 from the area still record seasonal, centennial and millennial scale variability in glacio-
 136 chemistry (Göktas et al., 2002; Oerter et al., 2000; Sommer et al., 2000), as well as highly-
 137 resolved tropical volcanic eruptions (Hofstede et al., 2004; Severi et al., 2007). This site
 138 offers useful potential to investigate the impact of volcanic eruptions on TCO, surface
 139 UV radiation and its imprint in the $\delta^{15}\text{N}(\text{NO}_3^-)$ ice core signature.

140 The aim of this study is to combine modelling studies with ice core evidence to un-
 141 derstand the impact on the total column ozone of explosive tropical volcanic eruptions
 142 in a low chlorine stratosphere. The first part of this study will explore the sensitivity of
 143 ozone over Antarctica to different volcanic emission scenarios using a state-of-the-art chemistry-
 144 climate model (UM-UKCA) with additional key heterogeneous and photolysis reactions.
 145 The second part of the study examines the $\delta^{15}\text{N}(\text{NO}_3^-)$ signal for the tropical volcanic
 146 eruption, Samalas. Section 2 described the methods used in this paper. We provide a
 147 brief overview of the UM-UKCA chemistry-climate model and the additional key het-
 148 erogeneous and photolysis reactions that were added to improved the representation of
 149 stratospheric ozone. A Pinatubo eruption test case is used to validate the response to
 150 a present day volcanic eruption. We also provide a brief description of the ice core data
 151 and the isotopic analysis. In Section 3.1, we use the model to investigate the response
 152 of stratospheric ozone to various volcanic emission scenarios in a pre-industrial atmo-
 153 sphere. The isotopic constraints offered on past ozone change from the ice core evidence
 154 are presented in Section 3.2. Finally, Section 4 combines the model results and ice core
 155 analysis to discuss the implications for past and future ozone changes from explosive trop-
 156 ical volcanoes.

157 2 Data and methods

158 2.1 Model description, changes

159 We make use of the coupled chemistry-climate model which consists of the United
 160 Kingdom Chemistry and Aerosol (UKCA) module together with the UK Met Office Uni-
 161 fied Model (UM) (Walters et al., 2019; Morgenstern et al., 2009; O’Connor et al., 2014).
 162 The model is free running and with prescribed sea ice and sea surface temperatures. The
 163 original configuration is similar to the Atmospheric Model Intercomparison Project (AMIP)
 164 simulation of UK Earth system model (UKESM) submission to the Coupled Model In-
 165 tercomparison Project Phase 6 (CMIP6) (Eyring et al., 2016). The resolution is 1.875°
 166 longitude by 1.25° latitude with 85 vertical levels extending from the surface to 85 km.
 167 The UKCA module is run with the combined stratosphere and troposphere chemistry
 168 (CheST) option at version 10.9. The model has an internally generated QBO and the
 169 dynamics of the stratosphere is well represented (Osprey et al., 2013). The model includes

170 the aerosol scheme, GLOMAP-mode, to simulate the direct and indirect radiative effects
 171 (Mann et al., 2010). Aerosol optical properties are computed online as the particle size
 172 distributions evolve due to micro-physical processes.

173 Stratospheric ozone concentrations are determined by sets of photo-chemical re-
 174 actions first described by Chapman (1930) plus ozone destroying catalytic cycles involv-
 175 ing chlorine, nitrogen, hydrogen and bromine radical species (Solomon, 1999). The pho-
 176 tolysis reactions in the model make use of rates calculated from a combination of the FAST-
 177 JX scheme (Wild et al., 2000; Bian & Prather, 2002; Neu et al., 2007) and look-up ta-
 178 bles. FAST-JX wavelengths range from 177 to 850 nm over 18 bins and calculates scat-
 179 tering for all bands (Telford et al., 2013). Above about 60 km, a look-up table of pho-
 180 tolysis rates (Lary & Pyle, 1991; Morgenstern et al., 2009) is used when wavelengths be-
 181 low 177 nm become important. Heterogeneous reactions are also important for deter-
 182 mining stratospheric ozone concentrations in the presence of polar stratospheric clouds
 183 in the polar lower stratosphere or in the presence of sulphate aerosol following explosive
 184 volcanic eruptions. Ozone depleting radicals are produced by the photolysis of the prod-
 185 ucts formed from halogen containing compounds reacting on the surface of stratospheric
 186 aerosol such as polar stratospheric clouds. These species include hydrochloric acid (HCl),
 187 chlorine nitrate (ClONO₂), hydrogen bromide (HBr) and bromine nitrate (BrONO₂).
 188 Three types of aerosol are considered by the model: ice, nitric acid trihydrate and sul-
 189 fate aerosol. Above a temperature of about 195 K, reactions occur on liquid sulfate aerosol,
 190 around 195 K to 188 K, the model forms nitric acid trihydrate particles and below about
 191 188 K, ice particles form.

192 We add 8 new heterogeneous reactions to the model involving chlorine and bromine
 193 species in a similar way to Dennison et al. (2019) with the main difference being the ex-
 194 plicit treatment of the reactions of 4 additional chemical species: Cl₂, Br₂, ClNO₂ and
 195 BrNO₂. These species are also photolysed to produce Cl and Br radicals. Reaction rates
 196 depend on the probability of a gas molecule colliding irreversibly with the surface of the
 197 aerosol and this is given by an uptake coefficient. We update the calculation of the up-
 198 take coefficients using the same scheme as Dennison et al. (2019) with the differences listed
 199 in Table A1 in the Appendix.

200 Klobas et al. (2017) show that stratospheric bromine from natural, very shortlived
 201 biogenic compounds is critically important in determining the sign of the ozone change
 202 from eruptions when stratospheric chlorine levels are low. Hence, we explicitly add the
 203 emissions of five very short-lived bromocarbon species (CH₃Br, CH₂BrCl, CH₂Br₂, CHBr₂Cl,
 204 CHBrCl₂). These represent estimates of pre-industrial natural emissions of the species
 205 (Yang et al., 2014) and are modified from Warwick et al. (2006). Further details of the
 206 model setup are described in Appendix A.

207 2.2 Model validation

208 The changes to the stratospheric chemistry are tested by running the model for 30
 209 years in a year 2000 time slice experiment using CMIP6 prescribed trace gases and sea
 210 surface temperature forcings. The model is mostly able to reproduce the observed to-
 211 tal column ozone and the results are similar to those found by Dennison et al. (2019) in
 212 which a more thorough discussion of the changes can be found. The improved match with
 213 observed TCO resulting from our model updates is shown in Figure 1(a). The spring ozone
 214 hole over Antarctica is deeper than the original model with total column ozone values
 215 reaching about 175 DU (65 to 90° S average) in October compared to about 200 DU in
 216 the original model. These values are closer to those in the ozone values from the satel-
 217 lite ozone dataset from the National Institute of Water and Atmospheric Research – Bodeker
 218 Scientific (NIWA-BS) satellite dataset (version 3.4; see <http://www.bodekerscientific.com/data/total-column-ozone>). The ozone hole minimum in the satellite data reaches
 219 about 185 DU although this happens earlier in September. The modified model still un-
 220

221 der predicts the summer ozone values which take longer to recover compared to obser-
 222 vations. This could be due to the vortex breakup being delayed and is a known issue in
 223 a number of comprehensive chemistry climate model (Eyring et al., 2010; Butchart et
 224 al., 2011; McLandress et al., 2012). Overall, our changes to the chemistry scheme lead
 225 to an ozone distribution that is very similar to Dennison et al. (2019).

226 To assess the model response to a volcanic perturbation in the present atmosphere
 227 we run an experiment that simulates the eruption of Mount Pinatubo. The model is first
 228 spun up using CMIP6 present day forcings, including changing trends in trace gases. We
 229 then initialize four ensemble runs using the climate state taken from four different years
 230 of the spun up model state. The runs use the CMIP6 trace gas forcings from 1979 to 1994
 231 with the eruption happening in 1991. Although the exact climate state at the time of
 232 the Pinatubo eruption is known from observations, the four ensemble runs are done so
 233 as to span over the variability arising from the QBO and ENSO. This allows the Pinatubo
 234 run to be compared to the pre-industrial volcanic runs in Section 3.1. The timing of his-
 235 torical volcanic eruptions is not well constrained and we do not know the phases of the
 236 QBO and ENSO in which the eruptions occurred. The ensemble is designed to average
 237 over this variability. We simulate the Pinatubo eruption as an emission of 10 Tg SO₂
 238 and 0.02 Tg HCl on 1 June 1991 into the stratosphere as a single vertical plume between
 239 19 and 24 km altitude (the neutral buoyancy height of the plume) at 15.1° N and 120.2°E.
 240 Mills et al. (2016) discuss the justification for various choices of modelling parameters
 241 for Pinatubo. The aim of this experiment is not to reproduce the observations after the
 242 Pinatubo eruption exactly but to check that, with the additional chemical reactions and
 243 emissions, our model is still able to simulate the broad pattern of the ozone response af-
 244 ter a current day explosive volcano.

245 Figure 1(b) shows change in total column ozone from the Pinatubo eruption in the
 246 NIWA-Bodeker dataset as the difference between a 1991 to 1994 average and a clima-
 247 tology taken from 1979 to 1990. Similarly, the same change in the model runs is shown
 248 in Figure 1(c) but using the average of the four ensemble runs. A non parametric per-
 249 mutation test is used to determine if the changes seen are larger than the natural vari-
 250 ability; changes below the level of the noise is represented by the grey fog which is plot-
 251 ted as overlaid contours at confidence levels of 95, 90, 80, 70 and 60%. The same test
 252 is used in all subsequent model plots. The red triangle marks the volcanic eruption in
 253 this and subsequent plots.

254 The initial, low latitude, increase in total column ozone south of the volcano in the
 255 year following the eruption and the decrease in ozone in Jan 1992 over the North Pole
 256 are captured by the model although the changes are shorter lived than in the satellite
 257 data. Note that the Antarctic ozone hole is not as prominent a feature in model runs
 258 due to the averaging of four ensemble members. Our model ozone changes are qualita-
 259 tively similar to the Pinatubo case study by Aquila et al. (2012) using a different chemistry-
 260 climate model. Aquila et al. (2012) also discuss, in more detail, the possible mechanisms
 261 for the stratospheric ozone changes. This experiment demonstrates that our modified
 262 model is able to satisfactorily stimulate the ozone changes associated with a present-day
 263 volcanic eruption.

264 2.3 Ice core analysis

265 The first high-resolution record of $\delta^{15}\text{N}(\text{NO}_3^-)$ was obtained for the last 1.3 kyr from
 266 the 120 m ISOL-ICE ice core. The core was drilled in the clean air sector at Kohnen Sta-
 267 tion, DML on the high-elevation East Antarctic Plateau (2892 m above sea-level; 74.9961° S, 0.094717° E)
 268 in January 2017. A full description of the methods for the ISOL-ICE ice core can be found
 269 in Winton et al. (2019) and only a brief summary is given here. The core was analysed
 270 for i) continuous flow analysis (CFA) of nitrate (NO_3^-), sodium (Na) and magnesium (Mg)
 271 mass concentrations and electrolytic meltwater conductivity at the British Antarctic Sur-

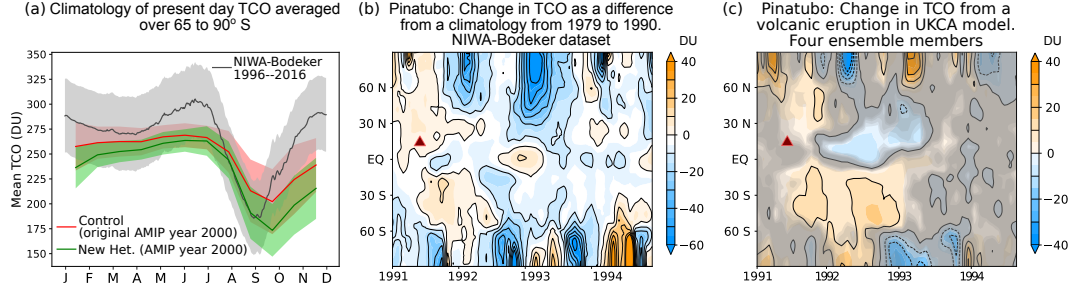


Figure 1. (a) Climatology of total column ozone (TCO) (DU) for the present climate from the NIWA-Bodeker satellite dataset (1996–2016) in black, a 30 year timeslice run of the year 2000 from the original AMIP model setup in red and the corresponding timeslice with the modified model with new heterogeneous reactions and emission files in green. Shaded bands show ± 1 standard deviation. (b) Change in Bodeker ozone following the Pinatubo eruption (red triangle) as a difference from a climatology taken from years 1979 to 1990. The QBO signal filtered out. (c) Change in TCO (DU) following a Pinatubo eruption (10 Tg SO_2 , 0.02 Tg HCl) in the model. The plot shows the difference from a climatology (1979 to 1990) and is the average of four ensemble members. The grey fog illustrates regions where the signal is below the level of the noise (see the main text for further details). The red triangle marks the volcanic eruption. Note the different colour scales between (b) and (c).

272 vey (BAS), Cambridge, and ii) discrete sections for the $\delta^{15}\text{N}(\text{NO}_3^-)$ composition at the
 273 Institute of Environmental Geosciences (IGE), University of Grenoble. Here we report
 274 the dated section of the ice core from 1227 to 1350 AD (69.8 to 79.4 m) covering the Samalás
 275 eruption in 1257. Dating was achieved by annual layer counting of measured concentra-
 276 tions of Na and Mg following previous studies at DML (Göktas et al., 2002; Weller &
 277 Wagenbach, 2007; Weller et al., 2008) constrained by well-dated volcanic horizons (fur-
 278 ther details can be found in Table B1). An age uncertainty of ± 3 years is estimated at
 279 the base of the ice core. High-resolution sampling for $\delta^{15}\text{N}(\text{NO}_3^-)$ analysis was carried
 280 out i) across volcanic horizons with a sample resolution of 5 to 30 cm, and ii) in 10 cm
 281 resolution baseline samples 1 m either side of the volcanic peak. A total of 119 discrete
 282 measurements of $\delta^{15}\text{N}(\text{NO}_3^-)$ are reported here. Discrete $\delta^{15}\text{N}(\text{NO}_3^-)$ samples were pre-
 283 concentrated and analysed using the denitrifier method following Frey et al. (2009) and
 284 Morin et al. (2009). The nitrogen isotopic ratio was referenced against N_2 -Air (Mariotti,
 285 1983). We report $^{15}\text{N}/^{14}\text{N}$ of NO_3^- ($\delta^{15}\text{N}(\text{NO}_3^-)$) as δ -values: $\delta^{15}\text{N}(\text{NO}_3^-) = 1000 \left(\frac{R_{\text{sample}}}{R_{\text{standard}}} - 1 \right)$
 286 where R is the elemental isotopic ratio in the sample and standard respectively. The over-
 287 all accuracy of the method for $\delta^{15}\text{N}(\text{NO}_3^-)$ is 3 per mil.

288 3 Results

289 3.1 Volcanic perturbations in model

290 Using the CMIP6 pre-industrial forcings, a year 1850 control run is produced. The
 291 control run is 60 years long excluding 10 years of spin up which are discarded. The ef-
 292 fect from explosive volcanoes on the stratosphere is investigated by running a series of
 293 four volcanic perturbation runs spun off from four different years of the control run to
 294 represent the variability arising from different ENSO and QBO states in a similar way
 295 to the Pinatubo case study in Section 2.2. The volcanic emissions are prescribed in a sim-
 296 ilar way to the Pinatubo eruption on 1 September of the first year of the run. Since his-
 297 torical volcanic eruptions are variable and HCl emissions are less well constrained, we
 298 develop a matrix of simulations that span the uncertainty in emissions. The six sets of

299 experiments have one of low SO₂ (10 Tg) or high SO₂ (100 Tg) paired with no HCl, low
 300 HCl (0.02 Tg) and high HCl (2 Tg). Changes are plotted as the difference between the
 301 average of the four perturbation runs and a climatology derived from the control run.

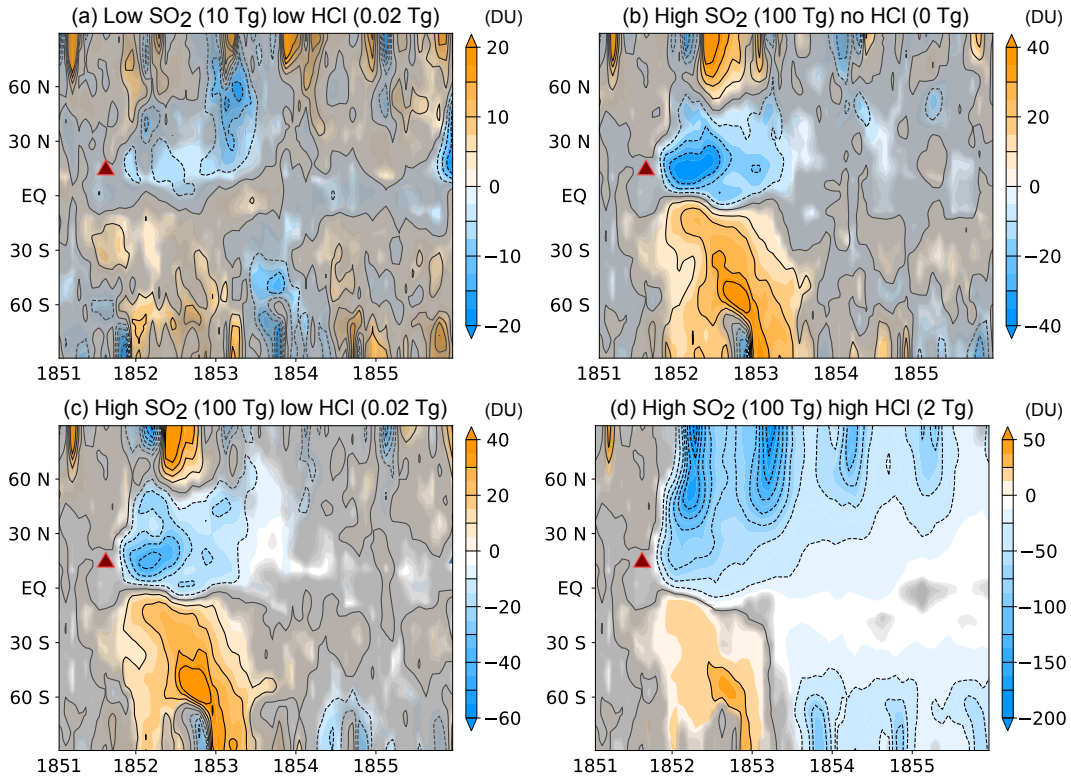


Figure 2. Change in total column ozone (DU) for the pre-industrial volcanic perturbation experiments. The plots show the difference between the average of four ensemble members and a single climatology drawn from a 60 year run. The emission scenarios shown are (a) low SO₂, low HCl case (b) high SO₂, no HCl (c) high SO₂, low HCl and (d) high SO₂, high HCl. The red triangle denotes the location of the injection. Note the different colour scales.

302 Figure 2 shows the change in total column ozone in the (a) low SO₂ + low HCl,
 303 (b) high SO₂ + no HCl, (c) high SO₂ + low HCl and (d) high SO₂ + high HCl cases.
 304 The low SO₂ + no HCl case and high SO₂ + no HCl cases are found to be qualitatively
 305 similar to two further experiments (not shown): the low SO₂ + low HCl and high SO₂
 306 + low HCl cases, respectively. This is expected since the stratospheric chlorine loading
 307 is low (< 0.4 ppbv of HCl over the polar region averaged between 65 to 90° S), as it is
 308 in a pre-industrial atmosphere. We do not observe large depletion of ozone depletion events
 309 by chlorine radicals during spring to form ozone holes.

310 The low SO₂ + low HCl case in Figure 2(a) represents the ozone response to a Pinatubo-
 311 like explosive volcano in a pre-industrial atmosphere. It shows that the changes in TCO
 312 are small and dominated by internal variability in most regions. This should be contrasted
 313 with the Pinatubo case study shown previously in Figure 1(c) where an eruption of an
 314 equivalent magnitude was able to cause significant ozone changes, including an ozone de-
 315 pletion of about 20 DU in the year following the eruption over Antarctica. In contrast,
 316 under scenarios of low or no HCl but when the SO₂ emitted is high (Figures 2(b) and
 317 (c)), substantial changes in total column ozone are seen for 1.5 years following the erup-
 318 tion. These two cases (high SO₂ and no HCl case, high SO₂ and low HCl) are qualita-

319 tively similar suggesting that transport effects still dominate when the amount of HCl
 320 is low in a pre-industrial atmosphere and the volcanic chlorine injection is not sufficient
 321 to make a significantly change the background stratospheric chlorine loading. The pri-
 322 mary impact of a large injection of SO₂ is to locally decrease TCO in the tropics and
 323 increase TCO at high latitudes, via the mechanisms described below.

324 Since chemical, dynamical and radiative processes are coupled in the model, it is
 325 difficult to quantify the contribution from individual processes but the results suggest
 326 that the main driver of the ozone changes is dynamical in the year following the erup-
 327 tion. The SO₂ aerosol leads to both longwave and shortwave heating in the lower strato-
 328 sphere (Robock, 2000) resulting in a change in the meridional circulation as shown in
 329 Figure 3(a). The increased upwelling brings more ozone-poor tropospheric air into the
 330 lower stratosphere leading to lower total column ozone. In contrast, the decreases in up-
 331 welling outside the initial SO₂ cloud results in an increase in ozone in the regions pole-
 332 wards of the SO₂ cloud in both hemispheres. Compared to the changes in transport, the
 333 changes to the partitioning between radicals and reservoir species for ClO_x, HO_x and
 334 NO_x appear to be a second order effect (not shown). The warming in the lower strato-
 335 sphere results in a warming of the cold point region. This region controls the freeze-drying
 336 of water vapour entering the lower stratosphere and warmer temperatures will result in
 337 a moistening of the stratosphere and subsequent changes to HO_x chemistry. Changes in
 338 SO₂ aerosol also change the partitioning between NO_y and N₂O₅ in the polar regions
 339 which can result in ozone changes but these have not been quantified in this study.

340 In contrast, when a substantial amount of HCl together with SO₂ is injected into
 341 the stratosphere (high SO₂ and high HCl case, Figure 2(d)), large, chemical ozone de-
 342 pletion occurs over the polar regions during spring time in the year two to four follow-
 343 ing the eruption. The initial, low latitude, response still appears to be dynamical but
 344 when the injected chlorine reaches polar regions (Figure 3(b)), catalytic destruction of
 345 ozone occurs in the polar vortex during spring. The mixing ratio of HCl reaches values
 346 of up to 4 ppbv and 1.3 ppbv at 20 km over the North and South poles respectively. These
 347 values are comparable to the present day (year 2000) values of the equivalent effective
 348 stratospheric chlorine of ~ 3 ppbv. The high SO₂ and high HCl scenario is the one ex-
 349 periment where we observed prolonged ozone destruction occurring over a number of years
 350 over Antarctica with a maximum decrease in total column ozone of ~ 90 DU in spring
 351 of the second year after the eruption. Over the North pole, stratospheric ozone is nearly
 352 completely removed in the spring for at least four years following the eruption.

353 The results are sensitive to the date, location and height of the injection in the trop-
 354 ics. A discussion of the sensitivity of eruption source parameters on volcanic radiative
 355 forcing can be found in Marshall et al. (2019). In our experiment, the lower branch of
 356 the Brewer-Dobson circulation is stronger in the Northern Hemisphere in September and
 357 hence the injected chlorine is primarily advected to the North pole in the months fol-
 358 lowing the eruption. It takes about 1.5 years for chlorine to be transported to the South
 359 pole. Our results are comparable to the experiments by Brenna et al. (2019) who im-
 360 pose a Central American explosive volcano in a chemistry climate model (CESM1) in
 361 which the effect of sulphuric acid aerosols are imposed as a modified El Chichòn surface
 362 area density forcing equivalent to 30 Mt SO₂. The results from their experiment with 2.93 Mt Cl,
 363 9.5 Mt Br at 14°N, 89°W with an injection height of 29.7 hPa on January 1 (their Fig-
 364 ure 3(c)) are qualitative similar to our results in Figure 2(d). Brenna et al. (2019) show
 365 that the average ozone decreases by more than 120 DU over the polar cap and observe
 366 a similar ozone increase over Antarctica in the year after that eruption which is followed
 367 by a series of four years with large spring-time ozone depletion. The duration of the re-
 368 sponse to a volcanic eruption is controlled by stratospheric dynamics and the material
 369 that is injected in the lower stratosphere is transported to the troposphere and removed
 370 within 2 to 5 years.

371 In summary, in a pre-industrial atmosphere with low chlorine levels in the strato-
 372 sphere, we do not detect a significant ozone response to a Pinatubo strength eruption
 373 in the model. A large explosive volcano, of similar magnitude to Samalas with no or low
 374 HCl produces an increase in total column ozone over Antarctica. The change is short-
 375 lived (~ 2 years) and primarily driven by transport changes. In contrast, if a volcanic
 376 injection of HCl (2 Tg in our experiments) is able to raise stratospheric chlorine concen-
 377 trations closer to present day levels, ozone depleting chemical reactions will occur to pro-
 378 duce Antarctic ozone depletion in spring as long as sufficient HCl is present. The strato-
 379 spheric lifetime of chlorine is determined by the age of air and the strength of the strato-
 380 spheric circulation. When the chlorine reaches the troposphere, it is washed out, giving
 381 a lifetime of about 5 years for HCl entering in the shallow branch of the Brewer-Dobson
 382 circulation. The increase in surface UV, resulting from ozone depletion, will affect the
 383 $\delta^{15}\text{N}(\text{NO}_3^-)$ ratio in the snow pack. The timing of the change in surface UV could lag,
 384 by a number of years, behind that of the volcanic sulphate signal in ice cores, since sul-
 385 phate arrives via tropospheric and stratospheric transport whilst the UV signal is de-
 386 pended on stratospheric ozone depletion. An additional difficulty is that the timing of
 387 the arrival of the signal depends on the season of the eruption; a quantity that is unknown
 388 for most volcanoes over the past 1000 years.

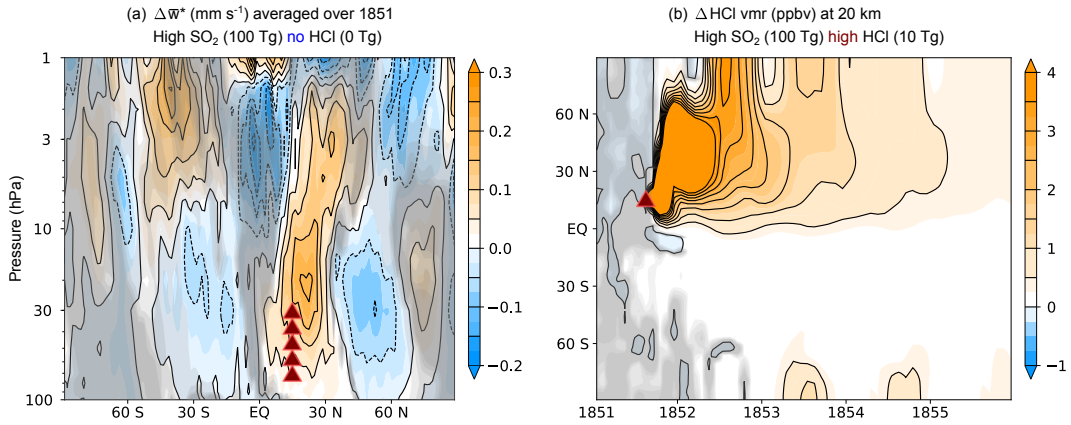


Figure 3. (a) Change in the mean residual vertical velocity averaged over one year after the eruption in the high SO₂ and no HCl case to show dynamical changes to the circulation. The red triangles represent the location and vertical extent of the volcanic eruption. (b) Change in HCl volume mixing ratio (ppbv) at 20 km for the high SO₂ and high HCl case to show chemical changes.

389 3.2 Ice core results

390 We expect a tropical volcanic eruption to lead to a sulphate signal in the ice record.
 391 The previous modelling studies show that high and high HCl eruptions can cause a
 392 decrease in TCO which would increase the UV dose reaching the surface at the ice core
 393 site. As a result, stronger photolysis would enhance NO₃⁻ loss, redistribution and recy-
 394 cling from snowpack, decreasing the NO₃⁻ mass concentration and enriching the $\delta^{15}\text{N}(\text{NO}_3^-)$
 395 signature.

396 The ISOL-ICE ice core data from 1227 to 1350 AD is illustrated in Figure 4. The
 397 ice core captures a clear signal of the 1257 Samalas series of four volcanic eruptions as
 398 indicated by elevated sulphate mass concentrations and electrolytic meltwater conduc-
 399 tivity levels above the background in the ice core (Figures 4(a) and (b)). This pattern
 400 is consistently observed in ice cores across DML and across the wider Antarctic re-

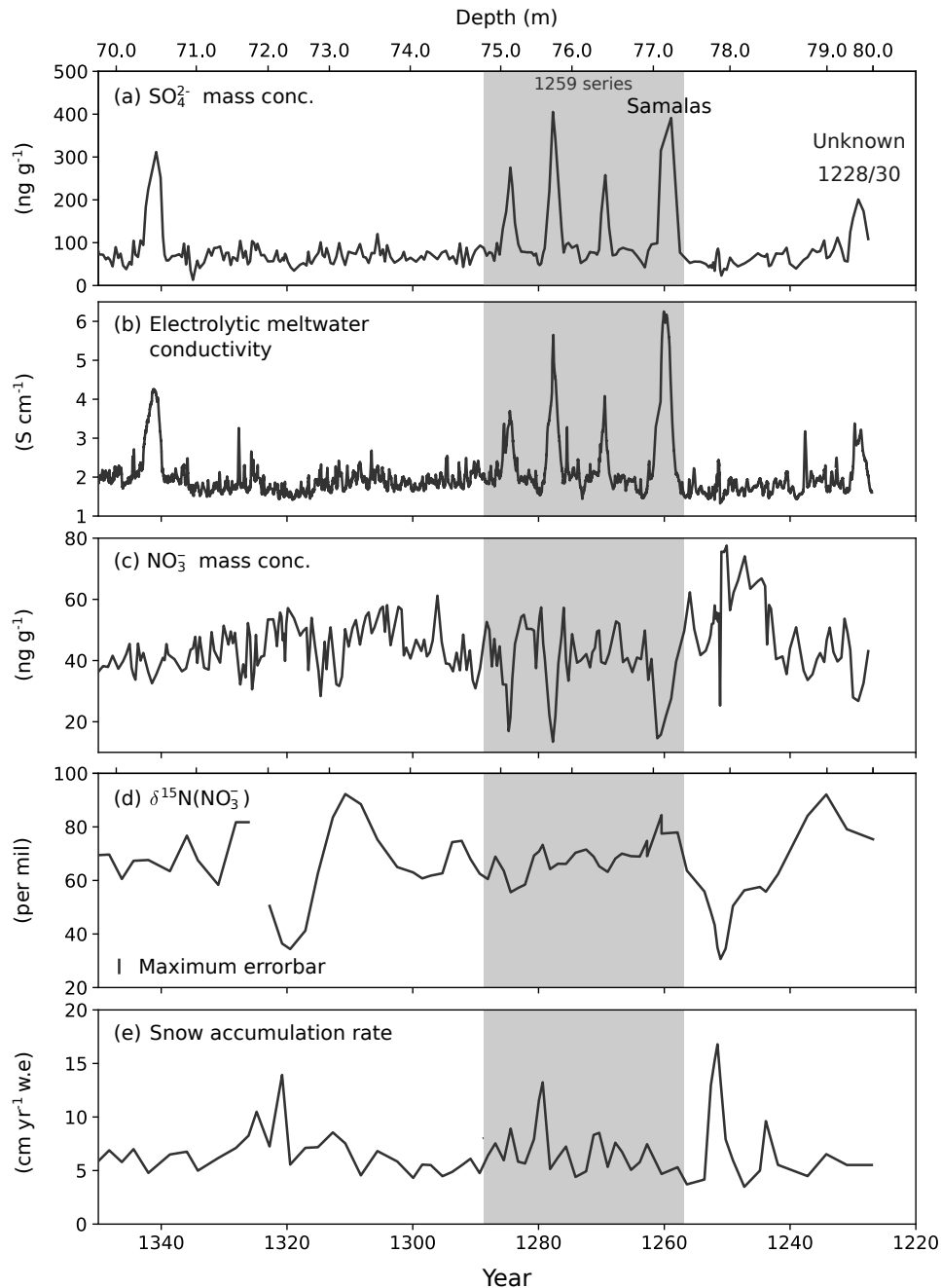


Figure 4. 1227 to 1350 AD section of the ISOL-ICE ice core data from DML, Antarctica. Age is plotted along the bottom and the corresponding ice depth along the top. The vertical grey region marks the dates around the 1257 series of volcanoes. (a) Sulphate mass concentrations. (b) Electrolytic melt water conductivity. (c) Nitrate mass concentration (d) Isotopic ratio of $^{15}\text{N}/^{14}\text{N}$ of NO_3^- ($\delta^{15}\text{N}(\text{NO}_3^-)$) given as δ -values. (e) Snow accumulation rate in (cm yr^{-1} water equivalent (w.e)). Note that the various quantities are available at different time resolutions depending on the analysis method used.

401 gion (e.g. Hofstede et al. (2004); Göktaş et al. (2002)), where sulphate originated from
 402 the 1257 series of eruptions, was transported via the stratosphere to Antarctica (Baroni

et al., 2008). Nitrate mass concentrations in the ice core decrease coincident with the four large volcanic eruptions (Figure 4(c)). This observation has been reported for other volcanic eruptions in Antarctic and Greenland ice cores, and is thought to occur from the displacement of NO_3^- in a highly acidic (sulphuric acid) volcanic layers (Wolff, 1995; Laj et al., 1993; Legrand & Kirchner, 1990). Based on other records of NO_3^- in Antarctica (Pasteris et al., 2014), we expect the NO_3^- mass concentration to be correlated to the accumulation rate. We do not see this positive correlation in the background variability in the ISOL-ICE ice core (Figure 4(c) and (e); $R^2 = 0.04, p < 10^{-3}$ with data from five years either side of the volcanic eruptions is not used). The $\delta^{15}\text{N}(\text{NO}_3^-)$ is weakly anti-correlated to the accumulation rate as would be expected from spatial transects across Antarctica (Figure 4(d) and (e); $R^2 = 0.2, p < 10^{-4}$ again with five years either side of the volcanic eruptions: w removed.) (Erbland et al., 2015, 2013; Noro et al., 2018; Shi et al., 2018), and sensitivity tests of variable accumulation rate on the $\delta^{15}\text{N}(\text{NO}_3^-)$ signal at the DML site (Winton et al., 2019).

The accumulation rate is variable at the DML site (2.5 to 11 cm yr^{-1} water equivalent) (Oerter et al., 2000; Sommer et al., 2000) and there is no trend over the last 1000 years. We speculate that changes in the accumulation rate will lead to changes in e-folding depth over time which can account for part of the variability of the $\delta^{15}\text{N}(\text{NO}_3^-)$ signal (Winton et al., 2019), with a smaller contribution from extreme precipitation events (Turner et al., 2019). The e-folding depth of the local snowpack depends on snow physical properties and contributes to the $\delta^{15}\text{N}(\text{NO}_3^-)$ signal eventually preserved in local firn and ice (Winton et al., 2019). Unfortunately, the variability of e-folding depth in the past is not known and may be a source of additional noise in the $\delta^{15}\text{N}(\text{NO}_3^-)$ signal.

We see no enrichment of the $\delta^{15}\text{N}(\text{NO}_3^-)$ signal above the background variability during the four volcanic eruptions Figure 4(d). We speculate on possible reasons for this lack of enrichment after the 1257 series. Firstly, the $\delta^{15}\text{N}(\text{NO}_3^-)$ UV proxy is not sensitive enough to record TCO and concurrent surface UV changes lasting only a few years. (Winton et al., 2019) assessed the sensitivity of the $\delta^{15}\text{N}(\text{NO}_3^-)$ UV proxy to changes in total column ozone using the TRANSITS model (Erbland et al., 2015). We expect that a decrease in the total column ozone of 100 DU, estimated for a large eruption on the magnitude of Samalás (assuming an eruption in September), would result in a 25 per mil increase in $\delta^{15}\text{N}(\text{NO}_3^-)$ at DML. However, this is below the inter-annual $\delta^{15}\text{N}(\text{NO}_3^-)$ variability of 30 to 90 per mil at DML (over the period 1227 to 1350 AD), and thus the development of a volcanic induced-large ozone depletion in spring is unlikely to be observed above the natural background $\delta^{15}\text{N}(\text{NO}_3^-)$ variability. Note that the inter-annual variability of $\delta^{15}\text{N}(\text{NO}_3^-)$ is larger than the seasonal variability of about ± 25 per mil of $\delta^{15}\text{N}(\text{NO}_3^-)$ seen at the bottom of the snow pits in Winton et al. (2019). Despite DML having a relatively low snow accumulation rate, the sensitivity of the $\delta^{15}\text{N}(\text{NO}_3^-)$ UV proxy is low at this site. Secondly, although we observe a significant decrease in the NO_3^- concentration during the volcanic eruptions, which could be attributed to NO_3^- loss from a stronger UV dose reaching the surface, we cannot rule out the possibility that the lower NO_3^- concentrations are due to migration of NO_3^- in acidic layers. Lastly, the impact of acidic volcanic layers on the $\delta^{15}\text{N}(\text{NO}_3^-)$ has yet to be quantified.

4 Discussion

The aim of this paper is to understand the impact on the total column ozone of explosive tropical volcanic eruptions in a low chlorine stratosphere and to search for evidence of these changes in the ice core record over the last 1000 years. We made use of the UM-UKCA chemistry-climate model, with improved heterogeneous reactions and emissions, to model the evolution of ozone after different injections scenarios of SO_2 and HCl representing possible past volcanic eruptions. We then compare the model results to the $\delta^{15}\text{N}(\text{NO}_3^-)$ isotopic ratio from the recently obtained ISOL-ICE ice core. Winton et al. (2019) and earlier work (Berhanu et al., 2015; Erbland et al., 2015) suggest that it may

455 be possible to use $\delta^{15}\text{N}(\text{NO}_3^-)$ as a UV proxy for Antarctic ozone changes, after account-
 456 ing for accumulation rate changes. A decrease in ozone leads to increased surface UV
 457 which increases the fractionation of $\delta^{15}\text{N}(\text{NO}_3^-)$ in the photolytically active region of the
 458 snowpack. The resulting $\delta^{15}\text{N}(\text{NO}_3^-)$ isotopic signal, which integrates the UV signal seen
 459 over several years, is then buried. We analyse the $\delta^{15}\text{N}(\text{NO}_3^-)$ ice core signature around
 460 the period of the Samalas eruption to reconstruct past UV changes.

461 The model experiments show that a ‘‘Pinatubo-like’’ eruption (low SO_2 , 10 Tg +
 462 low HCl, 0.02 Tg) in a pre-industrial atmosphere does not produce a significant response
 463 in ozone over Antarctica (Figure 2(c)) whilst the high SO_2 (100 Tg) volcanoes (with no
 464 or low HCl) both produce increases in ozone over Antarctica that are short-lived, last-
 465 ing about 1.5 years (Figure 2(b) and (c)). The pattern of ozone changes for the latter
 466 are primarily caused by transport changes arising from changes to the Brewer-Dobson
 467 circulation (Figure 3(a)). In contrast, when the amounts of SO_2 and HCl emitted are
 468 both high (high SO_2 , 100 Tg + high HCl, 2 Tg) and the HCl loading over the polar re-
 469 gions becomes comparable to present day stratospheric values, our model results show
 470 significant ozone depletion over both poles (Figure 2(d)) for at least four years follow-
 471 ing the eruption. Note that the chemical reactions that destroy ozone are only able to
 472 occur when HCl in the stratosphere reaches the polar regions and hence the timing of
 473 the springtime ozone depletion depends strongly on the date of the eruption. Since we
 474 model the eruption as occurring on 1 September, we find that it takes about 1 year for
 475 the injected HCl from the volcano to reach Antarctica (Figure 3(b)). Before the HCl reaches
 476 Antarctica, the increase in ozone over the Southern Hemisphere is caused by the same
 477 dynamical changes as in the low HCl model experiments.

478 The model experiments suggest that if a tropical volcano emits a substantial amount
 479 of SO_2 and HCl (high SO_2 , 100 Tg + high HCl, 2 Tg), prolonged ozone depletion, last-
 480 ing more than four years, will occur over Antarctica. We choose to focus on the ice core
 481 record around the Samalas eruption (part of the 1257 series of four volcanoes) since ice
 482 core and geochemical evidence suggests that this volcano was the largest in the past 1000
 483 years in terms of SO_2 and HCl emissions although there is significant uncertainty in the
 484 amount of HCl that was able to reach the stratosphere from this eruption (Halmer et
 485 al., 2002). The 1257 series of volcanoes that includes Samalas consists of four eruptions
 486 that occur at intervals of 10, 8 and 8 years. If all four eruptions caused ozone depletion,
 487 we expect to see a prolonged period of increase in $\delta^{15}\text{N}(\text{NO}_3^-)$ in the ice core.

488 Spatial transects across Antarctica (Noro et al., 2018, and references therein), sup-
 489 ported by air snow-photochemistry modelling (TRANSITS) (Winton et al., 2019; Erb-
 490 land et al., 2015) show a strong non linear dependence of $\delta^{15}\text{N}(\text{NO}_3^-)$ on snow accumu-
 491 lation rate which is not seen in the ice record (60–70 m depth). Deeper ice core records
 492 in Greenland have observed a dependence of $\delta^{15}\text{N}(\text{NO}_3^-)$ and accumulation rate on glacial-
 493 interglacial transition timescales (Freyer et al., 1996). However, in this paper, we present
 494 the highest resolution record in ice cores and do not observe a clear relationship on cen-
 495 tennial timescales. Our record of the isotopic ratio of $\delta^{15}\text{N}(\text{NO}_3^-)$ in the ice core around
 496 the 1257 series eruptions shows that using $\delta^{15}\text{N}(\text{NO}_3^-)$ as a proxy for ozone changes is
 497 inconclusive. Winton et al. (2019) show that for 100 DU change in total column ozone
 498 (Figure 2(d)), we expect to see a change of about 25 per mil in $\delta^{15}\text{N}(\text{NO}_3^-)$. This is be-
 499 low the level of inter-annual variability in $\delta^{15}\text{N}(\text{NO}_3^-)$ seen in the ice core of about 60
 500 to 90 per mil. The maximum uncertainty in our samples is less than ± 3 per mil over this
 501 time period. Note that the snow pack also integrates UV changes over a couple of years
 502 and smooths out seasonal variability. For a $\delta^{15}\text{N}(\text{NO}_3^-)$ signal to have been detected at
 503 the DML site from the 1257 eruptions, we suggest that it would require a prolonged pe-
 504 riod (several years) of near complete ozone destruction, for instance, during the series
 505 of seven stratospheric volcanic eruptions that occurred over a deglaciation ~ 17.7 ka (McConnell
 506 et al., 2017). With the additional caveat that the timing and magnitude of ozone changes
 507 depends on the season of the eruption, the climate model results suggest that this would

Reaction	Uptake coefficient		
	Ice	Nitric acid trihydrate	Sulphate aerosol
$\text{ClONO}_2 + \text{HCl} \rightarrow \text{Cl}_2 + \text{HNO}_3$	0.3	0.3	<i>f</i>
$\text{ClONO}_2 + \text{H}_2\text{O} \rightarrow \text{HOCl} + \text{HNO}_3$	0.3	0.006	<i>f</i>
$\text{HOCl} + \text{HCl} \rightarrow \text{Cl}_2 + \text{H}_2\text{O}$	0.3	0.3	<i>f</i>
$\text{N}_2\text{O}_5 + \text{H}_2\text{O} \rightarrow 2 \text{HNO}_3$	0.03	0.006	0.1
$\text{N}_2\text{O}_5 + \text{HCl} \rightarrow \text{ClNO}_2 + \text{HNO}_3$	0.03	0.006	0.02
$\text{HOBr} + \text{HCl} \rightarrow \text{BrCl} + \text{H}_2\text{O}$	0.25	0.25	0.1
$\text{BrONO}_2 + \text{HCl} \rightarrow \text{BrCl} + \text{HNO}_3$	0.3	0.3	0.01
$\text{BrONO}_2 + \text{H}_2\text{O} \rightarrow \text{HOBr} + \text{HNO}_3$	0.3	0.001	0.01
$\text{HOBr} + \text{HBr} \rightarrow \text{Br}_2 + \text{H}_2\text{O}$	0.25	0.25	0.1
$\text{HOCl} + \text{HBr} \rightarrow \text{BrCl} + \text{H}_2\text{O}$	0.25	0.25	0.02
$\text{ClONO}_2 + \text{HBr} \rightarrow \text{BrCl} + \text{HNO}_3$	0.56	0.56	0.02
$\text{BrONO}_2 + \text{HBr} \rightarrow \text{Br}_2 + \text{HNO}_3$	0.3	0.3	0.01
$\text{N}_2\text{O}_5 + \text{HBr} \rightarrow \text{BrNO}_2 + \text{HNO}_3$	0.05	0.001	0.02

f denotes uptake coefficients calculated using the method in Shi et al. (2001).

Table A1. New heterogeneous reactions added to the UKCA module together with the uptake coefficients.

508 require more than 2 Tg HCl to have been injected into the stratosphere. Since we do not
 509 see a $\delta^{15}\text{N}(\text{NO}_3^-)$ signal of this magnitude in the ice core, this provides a constraint on
 510 the magnitude of past ozone changes caused by the 1257 eruptions.

511 In summary, we have evaluated the impact of various explosive tropical volcanic
 512 emission scenarios on stratospheric ozone changes in a pre-industrial atmosphere and found
 513 that the sign of the ozone change over the polar regions depends on the amount of HCl
 514 injected by the eruption. $\delta^{15}\text{N}(\text{NO}_3^-)$ can theoretically be used as a proxy for UV and
 515 thus has the potential to indicate changes in past TCO. Changes in $\delta^{15}\text{N}(\text{NO}_3^-)$ could
 516 be positive or negative (indicating either increases or decreased in TCO) depending on
 517 the type of volcanic eruption and they are unlikely to be synchronous with sulphate peaks
 518 because of different transport pathways and the different timings of the ozone changes.
 519 Using a novel high resolution $\delta^{15}\text{N}(\text{NO}_3^-)$ ice core record, we are unable to detect a sig-
 520 nals from the largest volcanic eruption (1257 series) in the past 1000 years as there is a
 521 large inter-annual variability in the $\delta^{15}\text{N}(\text{NO}_3^-)$ record. We recommend that future stud-
 522 ies of this nature should first understand why the $\delta^{15}\text{N}(\text{NO}_3^-)$ record has a large vari-
 523 ability at DML site. A site with lower variability than 25 per mil in $\delta^{15}\text{N}(\text{NO}_3^-)$ could
 524 be considered although increasing the sensitivity of the UV proxy by choosing a site with
 525 lower annual accumulation comes at the expense of reduced time resolution making it
 526 less likely to resolve volcanic eruptions.

527 Appendix A Model improvements

528 A1 Heterogeneous and photolysis reactions

529 Table A1 lists the new heterogeneous reactions added to the UKCA module together
 530 with the uptake coefficients on ice, nitric acid trihydrate and sulfate aerosol. This can
 531 be compared to Table 1 in Dennison et al. (2019). We use the method in Shi et al. (2001)
 532 to calculate the values of the uptake coefficients that are not constant and are denoted
 533 by *f* in Table A1.

Volcano	Eruption date	Arrival date	Peak Depth (m)	Start Depth (m)
Kuwae ^a	1450	1454	61.01	61.13
1285 ^b	1285	1285	75.12	75.22
1277 ^b	1277	1277	75.77	75.9
1269 ^b	1269	1269	76.41	77.46
Samalas 1257 ^b	1257	1259	77.12	77.23
Unknown 1228/30 ^b	1229	1229	79.33	79.43

^a Zielinski et al. (1994) ^b Langway Jr. et al. (1995)

Table B1. Volcanic horizons identified from the sulfate and electrical meltwater conductivity records. Eruption date of the volcano and arrival dates of the sulfate in the ice core are obtained from Zielinski et al. (1994) and Langway Jr. et al. (1995) except for the Unknown 1228/30 volcano where the precise eruption date is not known. We choose 1229 as the eruption and arrival date for dating purposes.

534

A2 Bromocarbon emissions

535

536

537

538

539

540

541

542

The emission flux datasets of the five very short lived bromocarbon species (CH_3Br , CH_2BrCl , CH_2Br_2 , CHBr_2Cl , CHBrCl_2) are explicitly included as emission files. These are similar to the ones used in Yang et al. (2014), which are based on the original work (scenario 5) of Warwick et al. (2006), except for the emissions of CH_2Br_2 . The emissions of CH_2Br_2 were scaled to give a total emission of 57Gg yr^{-1} , corresponding to 50% of the original flux and in better agreement with Liang et al. (2010) and Ordóñez et al. (2012). The combined effect of the bromocarbons is to provide $\sim 5\text{pptv}$ of inorganic bromine to the stratosphere (Yang et al., 2014) in a pre-industrial atmosphere.

543

Appendix B Ice core analysis

544

545

Table B1 shows the volcanic horizons identified from the sulfate and electrical meltwater conductivity records in the ISOL-ICE ice core.

546

Acknowledgments

547

548

549

550

551

552

553

554

555

556

557

558

559

560

561

562

563

564

565

This project was funded by a National Environment Research Council (NERC) Standard Grant (NE/N011813/1) to MMF. VHLW would like to thank the University of Cambridge Doctoral Training Program (DTP) for funding a NERC Research Experience Project (REP) that contributed to this manuscript. JK received funding from the European Community's Seventh Framework Programme (FP7/2007-2013) under grant agreement no. 603557 (StratoClim). MD was supported by the Joint UK BEIS/Defra Met Office Hadley Centre Climate Programme (GA01101). AEJ was funded by the Natural Environment Research Council as part of British Antarctic Survey's programme "Polar Science for Planet Earth". NC thanks the ANR (Investissements d'avenir ANR-15-IDEX-02 and EAIIST grant ANR16-CE01-0011-01) and the INSU program LEFE-CHAT for supporting the stable isotope laboratory. This is a publication of the PANDA platform on which isotope analysis were performed. PANDA was partially funded by the LabEx OSUG@2020 (ANR10 LABX56). We would like to thank British Antarctic Survey (BAS) and Alfred Wegener Institute (AWI) staff for field and logistical support at Halley Station and Kohlen Station, respectively. Technical support for nitrate isotope analysis at the Institut des Géosciences de l'Environnement (IGE), Grenoble was provided by Pete Arkers. In addition, we thank Lisa Hauge, Emily Ludlow, Shaun Miller, Catriona Sinclair, Rebecca Tuckwell, Sarah Jackson, Julius Rix and Liz Thomas for technical support at BAS. We would like to thank Bodeker Scientific, funded by the New Zealand Deep South National

566 Science Challenge, for providing the combined NIWA-BS total column ozone database.
 567 The ice-core data set is available through the Polar Data Centre (Winton et al., 2019).
 568 This work used Monsoon2, a collaborative High Performance Computing facility funded
 569 by the Met Office and the Natural Environment Research Council. This work also used
 570 JASMIN, the UK collaborative data analysis facility. The model data is archived on the
 571 MONSooN2 platform and available upon request.

572 References

- 573 Aquila, V., Oman, L. D., Stolarski, R. S., Colarco, P. R., & Newman, P. A. (2012).
 574 Dispersion of the volcanic sulfate cloud from a mount pinatubolike erup-
 575 tion. *Journal of Geophysical Research: Atmospheres*, *117*(D6). Retrieved
 576 from [https://agupubs.onlinelibrary.wiley.com/doi/abs/10.1029/](https://agupubs.onlinelibrary.wiley.com/doi/abs/10.1029/2011JD016968)
 577 [2011JD016968](https://agupubs.onlinelibrary.wiley.com/doi/abs/10.1029/2011JD016968) doi: 10.1029/2011JD016968
- 578 Baroni, M., Savarino, J., Cole-Dai, J., Rai, V. K., & Thiemens, M. H. (2008).
 579 Anomalous sulfur isotope compositions of volcanic sulfate over the last millen-
 580 nium in antarctic ice cores. *Journal of Geophysical Research: Atmospheres*,
 581 *113*(D20). Retrieved from [https://agupubs.onlinelibrary.wiley.com/](https://agupubs.onlinelibrary.wiley.com/doi/abs/10.1029/2008JD010185)
 582 [doi/abs/10.1029/2008JD010185](https://agupubs.onlinelibrary.wiley.com/doi/abs/10.1029/2008JD010185) doi: 10.1029/2008JD010185
- 583 Berhanu, T. A., Meusinger, C., Erbland, J., Jost, R., Bhattacharya, S. K., John-
 584 son, M. S., & Savarino, J. (2014). Laboratory study of nitrate photolysis in
 585 antarctic snow. ii. isotopic effects and wavelength dependence. *The Journal*
 586 *of Chemical Physics*, *140*(24), 244306. Retrieved from [https://doi.org/](https://doi.org/10.1063/1.4882899)
 587 [10.1063/1.4882899](https://doi.org/10.1063/1.4882899) doi: 10.1063/1.4882899
- 588 Berhanu, T. A., Savarino, J., Erbland, J., Vicars, W. C., Preunkert, S., Martins,
 589 J. F., & Johnson, M. S. (2015). Isotopic effects of nitrate photochemistry in
 590 snow: a field study at dome c, antarctica. *Atmospheric Chemistry and Physics*,
 591 *15*(19), 11243–11256. Retrieved from [https://www.atmos-chem-phys.net/](https://www.atmos-chem-phys.net/15/11243/2015/)
 592 [15/11243/2015/](https://www.atmos-chem-phys.net/15/11243/2015/) doi: 10.5194/acp-15-11243-2015
- 593 Bian, H., & Prather, M. J. (2002, Mar 01). Fast-j2: Accurate simulation of
 594 stratospheric photolysis in global chemical models. *Journal of Atmospheric*
 595 *Chemistry*, *41*(3), 281–296. Retrieved from [https://doi.org/10.1023/A:](https://doi.org/10.1023/A:1014980619462)
 596 [1014980619462](https://doi.org/10.1023/A:1014980619462) doi: 10.1023/A:1014980619462
- 597 Brenna, H., Kutterolf, S., & Krger, K. (2019). Global ozone depletion and increase
 598 of UV radiation caused by pre-industrial tropical volcanic eruptions. *Scientific*
 599 *Reports*, *9*(1), 9435. doi: 10.1038/s41598-019-45630-0
- 600 Butchart, N., Charlton-Perez, A. J., Cionni, I., Hardiman, S. C., Haynes, P. H.,
 601 Krger, K., ... Yamashita, Y. (2011). Multimodel climate and variability of the
 602 stratosphere. *Journal of Geophysical Research: Atmospheres*, *116*(D5). doi:
 603 [10.1029/2010JD014995](https://doi.org/10.1029/2010JD014995)
- 604 Chapman, S. (1930). A theory of upper-atmospheric ozone. *Memories of Royal Me-*
 605 *teorological Society*, *III*(26), 103-125.
- 606 Dennison, F., Keeble, J., Morgenstern, O., Zeng, G., Abraham, N. L., & Yang, X.
 607 (2019). Improvements to stratospheric chemistry scheme in the um-ukca
 608 (v10.7) model: solar cycle and heterogeneous reactions. *Geoscientific Model*
 609 *Development*, *12*(3), 1227–1239. Retrieved from [https://www.geosci-model](https://www.geosci-model-dev.net/12/1227/2019/)
 610 [-dev.net/12/1227/2019/](https://www.geosci-model-dev.net/12/1227/2019/) doi: 10.5194/gmd-12-1227-2019
- 611 Erbland, J., Savarino, J., Morin, S., France, J. L., Frey, M. M., & King, M. D.
 612 (2015). Air-snow transfer of nitrate on the east antarctic plateau; part
 613 2: An isotopic model for the interpretation of deep ice-core records. *At-*
 614 *mospheric Chemistry and Physics*, *15*(20), 12079–12113. Retrieved from
 615 <https://www.atmos-chem-phys.net/15/12079/2015/> doi: 10.5194/
 616 [acp-15-12079-2015](https://www.atmos-chem-phys.net/15/12079/2015/)
- 617 Erbland, J., Vicars, W. C., Savarino, J., Morin, S., Frey, M. M., Frosini, D., ...
 618 Martins, J. M. F. (2013). Air-snow transfer of nitrate on the east antarctic

- 619 plateau; part 1: Isotopic evidence for a photolytically driven dynamic equi-
 620 librium in summer. *Atmospheric Chemistry and Physics*, 13(13), 6403–6419.
 621 Retrieved from <https://www.atmos-chem-phys.net/13/6403/2013/> doi:
 622 10.5194/acp-13-6403-2013
- 623 Eyring, V., Bony, S., Meehl, G. A., Senior, C. A., Stevens, B., Stouffer, R. J.,
 624 & Taylor, K. E. (2016). Overview of the coupled model intercompari-
 625 son project phase 6 (cmip6) experimental design and organization. *Geo-*
 626 *scientific Model Development*, 9(5), 1937–1958. Retrieved from [https://](https://www.geosci-model-dev.net/9/1937/2016/)
 627 www.geosci-model-dev.net/9/1937/2016/ doi: 10.5194/gmd-9-1937-2016
- 628 Eyring, V., Cionni, I., Bodeker, G. E., Charlton-Perez, A. J., Kinnison, D. E.,
 629 Scinocca, J. F., ... Yamashita, Y. (2010). Multi-model assessment of
 630 stratospheric ozone return dates and ozone recovery in ccmval-2 models.
 631 *Atmospheric Chemistry and Physics*, 10(19), 9451–9472. doi: 10.5194/
 632 acp-10-9451-2010
- 633 Frey, M. M., Savarino, J., Morin, S., Erbland, J., & Martins, J. M. F. (2009). Pho-
 634 tolysis imprint in the nitrate stable isotope signal in snow and atmosphere
 635 of east antarctica and implications for reactive nitrogen cycling. *Atmo-*
 636 *spheric Chemistry and Physics*, 9(22), 8681–8696. Retrieved from [https://](https://www.atmos-chem-phys.net/9/8681/2009/)
 637 www.atmos-chem-phys.net/9/8681/2009/ doi: 10.5194/acp-9-8681-2009
- 638 Freyer, H. D., Kobel, K., Delmas, R. J., Kley, D., & Legrand, M. R. (1996). First
 639 results of $^{15}\text{N}/^{14}\text{N}$ ratios in nitrate from alpine and polar ice cores. *Tellus B:*
 640 *Chemical and Physical Meteorology*, 48(1), 93–105. Retrieved from [https://](https://doi.org/10.3402/tellusb.v48i1.15671)
 641 doi.org/10.3402/tellusb.v48i1.15671 doi: 10.3402/tellusb.v48i1.15671
- 642 Göktas, F., Fischer, H., Oerter, H., Weller, R., Sommer, S., & Miller, H. (2002). A
 643 glacio-chemical characterization of the new epica deep-drilling site on amund-
 644 senisen, dronning maud land, antarctica. *Annals of Glaciology*, 35, 347–354.
 645 doi: 10.3189/172756402781816474
- 646 Halmer, M., Schmincke, H.-U., & Graf, H.-F. (2002). The annual volcanic gas input
 647 into the atmosphere, in particular into the stratosphere: a global data set for
 648 the past 100 years. *Journal of Volcanology and Geothermal Research*, 115(3),
 649 511 - 528. doi: [https://doi.org/10.1016/S0377-0273\(01\)00318-3](https://doi.org/10.1016/S0377-0273(01)00318-3)
- 650 Harris, N. R. P., Hassler, B., Tummon, F., Bodeker, G. E., Hubert, D.,
 651 Petropavlovskikh, I., ... Zawodny, J. M. (2015). Past changes in the vertical
 652 distribution of ozone part 3: Analysis and interpretation of trends. *Atmo-*
 653 *spheric Chemistry and Physics*, 15(17), 9965–9982. Retrieved from [https://](https://www.atmos-chem-phys.net/15/9965/2015/)
 654 www.atmos-chem-phys.net/15/9965/2015/ doi: 10.5194/acp-15-9965-2015
- 655 Hofstede, C. M., Roderik, S. v. d. W., Kaspers, K. A., van den Broeke, M. R.,
 656 Karlöf, L., Winther, J.-G., ... Wilhelms, F. (2004). Firn accumulation records
 657 for the past 1000 years on the basis of dielectric profiling of six cores from
 658 dronning maud land, antarctica. *Journal of Glaciology*, 50(169), 279–291. doi:
 659 10.3189/172756504781830169
- 660 Klobas, E. J., Wilmouth, D. M., Weisenstein, D. K., Anderson, J. G., & Salaw-
 661 itch, R. J. (2017). Ozone depletion following future volcanic eruptions.
 662 *Geophysical Research Letters*, 44(14), 7490–7499. Retrieved from [https://](https://agupubs.onlinelibrary.wiley.com/doi/abs/10.1002/2017GL073972)
 663 agupubs.onlinelibrary.wiley.com/doi/abs/10.1002/2017GL073972 doi:
 664 10.1002/2017GL073972
- 665 Kutterolf, S., Hansteen, T., Appel, K., Freundt, A., Krger, K., Prez, W., &
 666 Wehrmann, H. (2013, 06). Combined bromine and chlorine release from
 667 large explosive volcanic eruptions: A threat to stratospheric ozone? *Geology*,
 668 41(6), 707–710. Retrieved from <https://doi.org/10.1130/G34044.1> doi:
 669 10.1130/G34044.1
- 670 Laj, P., Palais, J. M., Gardner, J. E., & Sigurdsson, H. (1993, Apr 01). Modi-
 671 fied hno₃ seasonality in volcanic layers of a polar ice core: Snow-pack effect
 672 or photochemical perturbation? *Journal of Atmospheric Chemistry*, 16(3),
 673 219–230. Retrieved from <https://doi.org/10.1007/BF00696897> doi:

- 674 10.1007/BF00696897
- 675 Langematz, U., Tully (Lead authors), M., Calvo, N., Dameris, M., de Laat, A.,
676 Klekociuk, A., ... Young, P. (2018). Update on ozone-depleting substances
677 (odss) and other gases of interest to the montreal protocol. In *Scientific as-*
678 *essment of ozone depletion* (chap. 4). World Meteorological Organization,
679 Geneva, Switzerland.
- 680 Langway Jr., C. C., Osada, K., Clausen, H. B., Hammer, C. U., & Shoji, H. (1995).
681 A 10-century comparison of prominent bipolar volcanic events in ice cores.
682 *Journal of Geophysical Research: Atmospheres*, *100*(D8), 16241–16247.
683 Retrieved from [https://agupubs.onlinelibrary.wiley.com/doi/abs/](https://agupubs.onlinelibrary.wiley.com/doi/abs/10.1029/95JD01175)
684 [10.1029/95JD01175](https://agupubs.onlinelibrary.wiley.com/doi/abs/10.1029/95JD01175) doi: 10.1029/95JD01175
- 685 Lary, D. J., & Pyle, J. A. (1991, November). Diffuse radiation, twilight, and photo-
686 chemistry. I, II. *Journal of Atmospheric Chemistry*, *13*, 373–406. doi: 10.1007/
687 BF00057753
- 688 Legrand, M. R., & Kirchner, S. (1990). Origins and variations of nitrate in south
689 polar precipitation. *Journal of Geophysical Research: Atmospheres*, *95*(D4),
690 3493–3507. Retrieved from [https://agupubs.onlinelibrary.wiley.com/](https://agupubs.onlinelibrary.wiley.com/doi/abs/10.1029/JD095iD04p03493)
691 [doi/abs/10.1029/JD095iD04p03493](https://agupubs.onlinelibrary.wiley.com/doi/abs/10.1029/JD095iD04p03493) doi: 10.1029/JD095iD04p03493
- 692 Lehner, F., Schurer, A. P., Hegerl, G. C., Deser, C., & Frölicher, T. L. (2016).
693 The importance of enso phase during volcanic eruptions for detection and
694 attribution. *Geophysical Research Letters*, *43*(6), 2851–2858. Retrieved
695 from [https://agupubs.onlinelibrary.wiley.com/doi/abs/10.1002/](https://agupubs.onlinelibrary.wiley.com/doi/abs/10.1002/2016GL067935)
696 [2016GL067935](https://agupubs.onlinelibrary.wiley.com/doi/abs/10.1002/2016GL067935) doi: 10.1002/2016GL067935
- 697 Liang, Q., Stolarski, R. S., Kawa, S. R., Nielsen, J. E., Douglass, A. R., Rodriguez,
698 J. M., ... Ott, L. E. (2010). Finding the missing stratospheric br_y : a global
699 modeling study of $chbr_3$ and ch_2br_2 . *Atmospheric Chemistry and Physics*,
700 *10*(5), 2269–2286. Retrieved from [https://www.atmos-chem-phys.net/10/](https://www.atmos-chem-phys.net/10/2269/2010/)
701 [2269/2010/](https://www.atmos-chem-phys.net/10/2269/2010/) doi: 10.5194/acp-10-2269-2010
- 702 Mann, G. W., Carslaw, K. S., Spracklen, D. V., Ridley, D. A., Manktelow, P. T.,
703 Chipperfield, M. P., ... Johnson, C. E. (2010). Description and evaluation
704 of glomap-mode: a modal global aerosol microphysics model for the ukca
705 composition-climate model. *Geoscientific Model Development*, *3*(2), 519–551.
706 Retrieved from <https://www.geosci-model-dev.net/3/519/2010/> doi:
707 [10.5194/gmd-3-519-2010](https://www.geosci-model-dev.net/3/519/2010/)
- 708 Mariotti, A. (1983). Atmospheric nitrogen is a reliable standard for natural ^{15}N
709 abundance measurements. *Nature*, *303*(5919), 685–687. doi: [https://doi.org/](https://doi.org/10.1038/303685a0)
710 [10.1038/303685a0](https://doi.org/10.1038/303685a0)
- 711 Marshall, L., Johnson, J. S., Mann, G. W., Lee, L., Dhomse, S. S., Regayre, L.,
712 ... Schmidt, A. (2019). Exploring how eruption source parameters affect
713 volcanic radiative forcing using statistical emulation. *Journal of Geophys-*
714 *ical Research: Atmospheres*, *124*(2), 964–985. Retrieved from [https://](https://agupubs.onlinelibrary.wiley.com/doi/abs/10.1029/2018JD028675)
715 agupubs.onlinelibrary.wiley.com/doi/abs/10.1029/2018JD028675 doi:
716 [10.1029/2018JD028675](https://agupubs.onlinelibrary.wiley.com/doi/abs/10.1029/2018JD028675)
- 717 McConnell, J. R., Burke, A., Dunbar, N. W., Köhler, P., Thomas, J. L., Arienzo,
718 M. M., ... Winckler, G. (2017). Synchronous volcanic eruptions and abrupt
719 climate change ~17.7 ka plausibly linked by stratospheric ozone depletion.
720 *Proceedings of the National Academy of Sciences*, *114*(38), 10035–10040. doi:
721 [10.1073/pnas.1705595114](https://doi.org/10.1073/pnas.1705595114)
- 722 McLandress, C., Shepherd, T. G., Polavarapu, S., & Beagley, S. R. (2012). Is miss-
723 ing orographic gravity wave drag near 60s the cause of the stratospheric zonal
724 wind biases in chemistryclimate models? *Journal of the Atmospheric Sciences*,
725 *69*(3), 802–818. doi: 10.1175/JAS-D-11-0159.1
- 726 Mills, M. J., Schmidt, A., Easter, R., Solomon, S., Kinnison, D. E., Ghan, S. J.,
727 ... Gettelman, A. (2016). Global volcanic aerosol properties derived
728 from emissions, 1990–2014, using cesm1(waccm). *Journal of Geophysi-*

- 729 *cal Research: Atmospheres*, 121(5), 2332–2348. Retrieved from [https://](https://agupubs.onlinelibrary.wiley.com/doi/abs/10.1002/2015JD024290)
730 agupubs.onlinelibrary.wiley.com/doi/abs/10.1002/2015JD024290 doi:
731 10.1002/2015JD024290
- 732 Morgenstern, O., Braesicke, P., O’Connor, F. M., Bushell, A. C., Johnson, C. E.,
733 Osprey, S. M., & Pyle, J. A. (2009). Evaluation of the new ukca climate-
734 composition model; part 1: The stratosphere. *Geoscientific Model Develop-*
735 *ment*, 2(1), 43–57. Retrieved from [https://www.geosci-model-dev.net/2/](https://www.geosci-model-dev.net/2/43/2009/)
736 43/2009/ doi: 10.5194/gmd-2-43-2009
- 737 Morin, S., Savarino, J., Frey, M. M., Domine, F., Jacobi, H.-W., Kaleschke, L., &
738 Martins, J. M. F. (2009). Comprehensive isotopic composition of atmospheric
739 nitrate in the atlantic ocean boundary layer from 65°s to 79°n. *Journal of*
740 *Geophysical Research: Atmospheres*, 114(D5). Retrieved from [https://](https://agupubs.onlinelibrary.wiley.com/doi/abs/10.1029/2008JD010696)
741 agupubs.onlinelibrary.wiley.com/doi/abs/10.1029/2008JD010696 doi:
742 10.1029/2008JD010696
- 743 Neu, J. L., Prather, M. J., & Penner, J. E. (2007). Global atmospheric chemistry:
744 Integrating over fractional cloud cover. *Journal of Geophysical Research: At-*
745 *mospheres*, 112(D11). Retrieved from [https://agupubs.onlinelibrary](https://agupubs.onlinelibrary.wiley.com/doi/abs/10.1029/2006JD008007)
746 [.wiley.com/doi/abs/10.1029/2006JD008007](https://agupubs.onlinelibrary.wiley.com/doi/abs/10.1029/2006JD008007) doi: 10.1029/2006JD008007
- 747 Noro, K., Hattori, S., Uemura, R., Fukui, K., Hirabayashi, M., Kawamura, K.,
748 ... Yoshida, N. (2018). Spatial variation of isotopic compositions of snow-
749 pack nitrate related to post-depositional processes in eastern dronning maud
750 land, east antarctica. *GEOCHEMICAL JOURNAL*, 52(2), e7–e14. doi:
751 10.2343/geochemj.2.0519
- 752 O’Connor, F. M., Johnson, C. E., Morgenstern, O., Abraham, N. L., Braesicke,
753 P., Dalvi, M., ... Pyle, J. A. (2014). Evaluation of the new ukca climate-
754 composition model – part 2: The troposphere. *Geoscientific Model Develop-*
755 *ment*, 7(1), 41–91. doi: 10.5194/gmd-7-41-2014
- 756 Oerter, H., Wilhelms, F., Jung-Rothenhäusler, F., Göktaş, F., Miller, H., Graf, W.,
757 & Sommer, S. (2000). Accumulation rates in dronning maud land, antarctica,
758 as revealed by dielectric-profiling measurements of shallow firn cores. *Annals of*
759 *Glaciology*, 30, 2734. doi: 10.3189/172756400781820705
- 760 Ordóñez, C., Lamarque, J.-F., Tilmes, S., Kinnison, D. E., Atlas, E. L., Blake,
761 D. R., ... Saiz-Lopez, A. (2012). Bromine and iodine chemistry in a global
762 chemistry-climate model: description and evaluation of very short-lived
763 oceanic sources. *Atmospheric Chemistry and Physics*, 12(3), 1423–1447.
764 Retrieved from <https://www.atmos-chem-phys.net/12/1423/2012/> doi:
765 10.5194/acp-12-1423-2012
- 766 Osprey, S. M., Gray, L. J., Hardiman, S. C., Butchart, N., & Hinton, T. J. (2013).
767 Stratospheric variability in twentieth-century cmip5 simulations of the met
768 office climate model: High top versus low top. *Journal of Climate*, 26(5),
769 1595–1606. Retrieved from <https://doi.org/10.1175/JCLI-D-12-00147.1>
770 doi: 10.1175/JCLI-D-12-00147.1
- 771 Pasteris, D., McConnell, J. R., Edwards, R., Isaksson, E., & Albert, M. R. (2014).
772 Acidity decline in antarctic ice cores during the little ice age linked to changes
773 in atmospheric nitrate and sea salt concentrations. *Journal of Geophys-*
774 *ical Research: Atmospheres*, 119(9), 5640–5652. Retrieved from [https://](https://agupubs.onlinelibrary.wiley.com/doi/abs/10.1002/2013JD020377)
775 agupubs.onlinelibrary.wiley.com/doi/abs/10.1002/2013JD020377 doi:
776 10.1002/2013JD020377
- 777 Poberaj, C. S., Staehelin, J., & Brunner, D. (2011). Missing stratospheric ozone
778 decrease at southern hemisphere middle latitudes after mt. pinatubo: A
779 dynamical perspective. *Journal of the Atmospheric Sciences*, 68(9), 1922–
780 1945. Retrieved from <https://doi.org/10.1175/JAS-D-10-05004.1> doi:
781 10.1175/JAS-D-10-05004.1
- 782 Robock, A. (2000). Volcanic eruptions and climate. *Reviews of Geophysics*, 38(2),
783 191–219. Retrieved from <https://agupubs.onlinelibrary.wiley.com/doi/>

- 784 abs/10.1029/1998RG000054 doi: 10.1029/1998RG000054
 785 Robock, A., & Oppenheimer, C. (Eds.). (2003). *Volcanism and the Earth's Atmo-*
 786 *sphere* (Vol. 139). Washington DC American Geophysical Union Geophysical
 787 Monograph Series. doi: 10.1029/GM139
- 788 Severi, M., Becagli, S., Castellano, E., Morganti, A., Traversi, R., Udisti, R., ...
 789 Steffensen, J. P. (2007). Synchronisation of the edml and edc ice cores for
 790 the last 52 kyr by volcanic signature matching. *Climate of the Past*, 3(3),
 791 367–374. Retrieved from <https://www.clim-past.net/3/367/2007/> doi:
 792 10.5194/cp-3-367-2007
- 793 Shi, G., Buffen, A., Ma, H., Hu, Z., Sun, B., Li, C., ... Hastings, M. (2018). Distinguishing summertime atmospheric production of nitrate across the east antarctic ice sheet. *Geochimica et Cosmochimica Acta*, 231, 1 - 14. Retrieved from <http://www.sciencedirect.com/science/article/pii/S0016703718301856> doi: <https://doi.org/10.1016/j.gca.2018.03.025>
- 794 Shi, G., Chai, J., Zhu, Z., Hu, Z., Chen, Z., Yu, J., ... Hastings, M. (2019). Iso-
 795 tope fractionation of nitrate during volatilization in snow: A field investigation
 796 in antarctica. *Geophysical Research Letters*, 46(6), 3287–3297. Retrieved
 797 from [https://agupubs.onlinelibrary.wiley.com/doi/abs/10.1029/](https://agupubs.onlinelibrary.wiley.com/doi/abs/10.1029/2019GL081968)
 798 2019GL081968 doi: 10.1029/2019GL081968
- 800 Shi, Q., Jayne, J. T., Kolb, C. E., Worsnop, D. R., & Davidovits, P. (2001). Kinetic
 801 model for reaction of clono2 with h2o and hcl and hocl with hcl in sulfuric acid
 802 solutions. *Journal of Geophysical Research: Atmospheres*, 106(D20), 24259-
 803 24274. Retrieved from [https://agupubs.onlinelibrary.wiley.com/doi/](https://agupubs.onlinelibrary.wiley.com/doi/abs/10.1029/2000JD000181)
 804 [abs/10.1029/2000JD000181](https://agupubs.onlinelibrary.wiley.com/doi/abs/10.1029/2000JD000181) doi: 10.1029/2000JD000181
- 805 Solomon, S. (1999). Stratospheric ozone depletion: A review of concepts and history. *Reviews of Geophysics*, 37(3), 275-316. Retrieved from [https://agupubs](https://agupubs.onlinelibrary.wiley.com/doi/abs/10.1029/1999RG900008)
 806 [.onlinelibrary.wiley.com/doi/abs/10.1029/1999RG900008](https://agupubs.onlinelibrary.wiley.com/doi/abs/10.1029/1999RG900008) doi: 10.1029/
 807 1999RG900008
- 808 Sommer, S., Appenzeller, C., Röthlisberger, R., Hutterli, M. A., Stauffer, B.,
 809 Wagenbach, D., ... Mulvaney, R. (2000). Glacio-chemical study span-
 810 ning the past 2 kyr on three ice cores from dronning maud land, antar-
 811 ctica: 1. annually resolved accumulation rates. *Journal of Geophysical Re-*
 812 *search: Atmospheres*, 105(D24), 29411-29421. Retrieved from [https://](https://agupubs.onlinelibrary.wiley.com/doi/abs/10.1029/2000JD900449)
 813 agupubs.onlinelibrary.wiley.com/doi/abs/10.1029/2000JD900449 doi:
 814 10.1029/2000JD900449
- 815 Sommer, S., Wagenbach, D., Mulvaney, R., & Fischer, H. (2000). Glacio-chemical
 816 study spanning the past 2 kyr on three ice cores from dronning maud land,
 817 antarctica: 2. seasonally resolved chemical records. *Journal of Geophysical*
 818 *Research: Atmospheres*, 105(D24), 29423-29433. Retrieved from [https://](https://agupubs.onlinelibrary.wiley.com/doi/abs/10.1029/2000JD900450)
 819 agupubs.onlinelibrary.wiley.com/doi/abs/10.1029/2000JD900450 doi:
 820 10.1029/2000JD900450
- 821 Stevenson, S., Fasullo, J. T., Otto-Bliesner, B. L., Tomas, R. A., & Gao, C. (2017).
 822 Role of eruption season in reconciling model and proxy responses to tropical
 823 volcanism. *Proceedings of the National Academy of Sciences*, 114(8), 1822–
 824 1826. Retrieved from <https://www.pnas.org/content/114/8/1822> doi:
 825 10.1073/pnas.1612505114
- 826 Telford, P., Braesicke, P., Morgenstern, O., & Pyle, J. (2009). Reassessment of
 827 causes of ozone column variability following the eruption of mount pinatubo
 828 using a nudged ccm. *Atmospheric Chemistry and Physics*, 9(13), 4251–4260.
 829 Retrieved from <https://www.atmos-chem-phys.net/9/4251/2009/> doi:
 830 10.5194/acp-9-4251-2009
- 831 Telford, P. J., Abraham, N. L., Archibald, A. T., Braesicke, P., Dalvi, M., Mor-
 832 genstern, O., ... Pyle, J. A. (2013). Implementation of the fast-jx pho-
 833 tolysis scheme (v6.4) into the ukca component of the metum chemistry-
 834 climate model (v7.3). *Geoscientific Model Development*, 6(1), 161–177.

- 839 Retrieved from <https://www.geosci-model-dev.net/6/161/2013/> doi:
840 10.5194/gmd-6-161-2013
- 841 Textor, C., Graf, H.-F., Herzog, M., & Oberhuber, J. M. (2003). Injection of
842 gases into the stratosphere by explosive volcanic eruptions. *Journal of*
843 *Geophysical Research: Atmospheres*, 108(D19). Retrieved from [https://](https://agupubs.onlinelibrary.wiley.com/doi/abs/10.1029/2002JD002987)
844 agupubs.onlinelibrary.wiley.com/doi/abs/10.1029/2002JD002987 doi:
845 10.1029/2002JD002987
- 846 Theys, N., De Smedt, I., Van Roozendael, M., Froidevaux, L., Clarisse, L., & Hen-
847 drick, F. (2014). First satellite detection of volcanic ocló after the eruption
848 of puyehue-cordón caulle. *Geophysical Research Letters*, 41(2), 667–672.
849 Retrieved from [https://agupubs.onlinelibrary.wiley.com/doi/abs/](https://agupubs.onlinelibrary.wiley.com/doi/abs/10.1002/2013GL058416)
850 [10.1002/2013GL058416](https://agupubs.onlinelibrary.wiley.com/doi/abs/10.1002/2013GL058416) doi: 10.1002/2013GL058416
- 851 Tie, X., & Brasseur, G. (1995). The response of stratospheric ozone to volcanic
852 eruptions: Sensitivity to atmospheric chlorine loading. *Geophysical Research*
853 *Letters*, 22, 3035–3038. doi: 10.1029/95GL03057
- 854 Timmreck, C., Mann, G. W., Aquila, V., Hommel, R., Lee, L. A., Schmidt,
855 A., ... Weisenstein, D. (2018). The interactive stratospheric aerosol
856 model intercomparison project (isa-mip): motivation and experimen-
857 tal design. *Geoscientific Model Development*, 11(7), 2581–2608. Re-
858 trieved from <https://www.geosci-model-dev.net/11/2581/2018/> doi:
859 10.5194/gmd-11-2581-2018
- 860 Toohey, M., & Sigl, M. (2017). Volcanic stratospheric sulfur injections and aerosol
861 optical depth from 500 bce to 1900 ce. *Earth System Science Data*, 9(2), 809–
862 831. Retrieved from <https://www.earth-syst-sci-data.net/9/809/2017/>
863 doi: 10.5194/essd-9-809-2017
- 864 Turner, J., Phillips, T., Thamban, M., Rahaman, W., Marshall, G. J., Wille, J. D.,
865 ... Lachlan-Cope, T. (2019). The dominant role of extreme precipitation
866 events in antarctic snowfall variability. *Geophysical Research Letters*, 46(6),
867 3502–3511. Retrieved from [https://agupubs.onlinelibrary.wiley.com/](https://agupubs.onlinelibrary.wiley.com/doi/abs/10.1029/2018GL081517)
868 [doi/abs/10.1029/2018GL081517](https://agupubs.onlinelibrary.wiley.com/doi/abs/10.1029/2018GL081517) doi: 10.1029/2018GL081517
- 869 Vidal, C. M., Métrich, N., Komorowski, J.-C., Pratomo, I., Michel, A., Kartadinata,
870 N., ... Lavigne, F. (2016, October). The 1257 samalas eruption (lombok,
871 indonesia): the single greatest stratospheric gas release of the common era.
872 *Scientific reports*, 6, 34868. doi: 10.1038/srep34868
- 873 Wallace, L., & Livingston, W. (1992). The effect of the pinatubo cloud on hydrogen
874 chloride and hydrogen fluoride. *Geophysical Research Letters*, 19(12), 1209–
875 1209. Retrieved from [https://agupubs.onlinelibrary.wiley.com/doi/abs/](https://agupubs.onlinelibrary.wiley.com/doi/abs/10.1029/92GL01112)
876 [10.1029/92GL01112](https://agupubs.onlinelibrary.wiley.com/doi/abs/10.1029/92GL01112) doi: 10.1029/92GL01112
- 877 Walters, D., Baran, A. J., Boutle, I., Brooks, M., Earnshaw, P., Edwards, J., ...
878 Zerroukat, M. (2019). The met office unified model global atmosphere 7.0/7.1
879 and jules global land 7.0 configurations. *Geoscientific Model Development*,
880 12(5), 1909–1963. doi: 10.5194/gmd-12-1909-2019
- 881 Warwick, N. J., Pyle, J. A., Carver, G. D., Yang, X., Savage, N. H., O’Connor,
882 F. M., & Cox, R. A. (2006). Global modeling of biogenic bromocar-
883 bons. *Journal of Geophysical Research: Atmospheres*, 111(D24). Retrieved
884 from [https://agupubs.onlinelibrary.wiley.com/doi/abs/10.1029/](https://agupubs.onlinelibrary.wiley.com/doi/abs/10.1029/2006JD007264)
885 [2006JD007264](https://agupubs.onlinelibrary.wiley.com/doi/abs/10.1029/2006JD007264) doi: 10.1029/2006JD007264
- 886 Weller, R., & Wagenbach, D. (2007). Year-round chemical aerosol records in con-
887 tinental antarctica obtained by automatic samplings. *Tellus B: Chemical and*
888 *Physical Meteorology*, 59(4), 755–765. Retrieved from [https://doi.org/](https://doi.org/10.1111/j.1600-0889.2007.00293.x)
889 [10.1111/j.1600-0889.2007.00293.x](https://doi.org/10.1111/j.1600-0889.2007.00293.x) doi: 10.1111/j.1600-0889.2007.00293.x
- 890 Weller, R., Wöltjen, J., Piel, C., Resenberg, R., Wagenbach, D., König-Langlo, G., &
891 Kriews, M. (2008). Seasonal variability of crustal and marine trace elements in
892 the aerosol at neumayer station, antarctica. *Tellus B: Chemical and Physical*
893 *Meteorology*, 60(5), 742–752. Retrieved from <https://doi.org/10.1111/>

- 894 j.1600-0889.2008.00372.x doi: 10.1111/j.1600-0889.2008.00372.x
 895 Wild, O., Zhu, X., & Prather, M. J. (2000, Nov 01). Fast-j: Accurate simulation
 896 of in- and below-cloud photolysis in tropospheric chemical models. *Journal of*
 897 *Atmospheric Chemistry*, *37*(3), 245–282. Retrieved from [https://doi.org/10](https://doi.org/10.1023/A:1006415919030)
 898 [.1023/A:1006415919030](https://doi.org/10.1023/A:1006415919030) doi: 10.1023/A:1006415919030
- 899 Winton, V. H. L., Ming, A., Caillon, N., Hauge, L., Jones, A. E., Savarino, J., ...
 900 Frey, M. M. (2019). Deposition, recycling and archival of nitrate stable iso-
 901 totes between the air-snow interface: comparison between dronning maud land
 902 and dome c, antarctica. *Atmospheric Chemistry and Physics Discussions*,
 903 *2019*, 1–44. Retrieved from [https://www.atmos-chem-phys-discuss.net/](https://www.atmos-chem-phys-discuss.net/acp-2019-669/)
 904 [acp-2019-669/](https://www.atmos-chem-phys-discuss.net/acp-2019-669/) doi: 10.5194/acp-2019-669
- 905 Winton, V. H. L. W., Caillon, N., Hauge, L., Mulvaney, R., Rix, J., Savarino, J.,
 906 ... Frey, M. (2019). *Ice core chemistry, conductivity, and stable nitrate iso-*
 907 *topic composition of the samalas eruption in 1259 from the isol-ice ice core,*
 908 *dronning maud land, antarctica, version 1.0.* [https://doi.org/10.5285/](https://doi.org/10.5285/d9a74ea7-2a1a-4068-847e-5bc9f51947c5)
 909 [d9a74ea7-2a1a-4068-847e-5bc9f51947c5](https://doi.org/10.5285/d9a74ea7-2a1a-4068-847e-5bc9f51947c5). UK Polar Data Centre, Nat-
 910 ural Environment Research Council, UK Research and Innovation. doi:
 911 [10.5285/d9a74ea7-2a1a-4068-847e-5bc9f51947c5](https://doi.org/10.5285/d9a74ea7-2a1a-4068-847e-5bc9f51947c5)
- 912 Wolff, E. W. (1995). Nitrate in polar ice. In R. J. Delmas (Ed.), *Ice core studies of*
 913 *global biogeochemical cycles* (pp. 195–224). Berlin: Springer-Verlag. Retrieved
 914 from <http://nora.nerc.ac.uk/id/eprint/515900/>
- 915 Yang, X., Abraham, N. L., Archibald, A. T., Braesicke, P., Keeble, J., Telford,
 916 P. J., ... Pyle, J. A. (2014). How sensitive is the recovery of strato-
 917 spheric ozone to changes in concentrations of very short-lived bromocar-
 918 bons? *Atmospheric Chemistry and Physics*, *14*(19), 10431–10438. Re-
 919 trieved from <https://www.atmos-chem-phys.net/14/10431/2014/> doi:
 920 [10.5194/acp-14-10431-2014](https://www.atmos-chem-phys.net/14/10431/2014/)
- 921 Zanchettin, D., Khodri, M., Timmreck, C., Toohey, M., Schmidt, A., Gerber, E. P.,
 922 ... Tummon, F. (2016). The model intercomparison project on the cli-
 923 matic response to volcanic forcing (volmip): experimental design and forcing
 924 input data for cmip6. *Geoscientific Model Development*, *9*(8), 2701–2719.
 925 Retrieved from <https://www.geosci-model-dev.net/9/2701/2016/> doi:
 926 [10.5194/gmd-9-2701-2016](https://www.geosci-model-dev.net/9/2701/2016/)
- 927 Zielinski, G. A., Mayewski, P. A., Meeker, L. D., Whitlow, S., Twickler, M. S., Mor-
 928 rison, M., ... Alley, R. B. (1994). Record of volcanism since 7000 b.c. from
 929 the gisp2 greenland ice core and implications for the volcano-climate system.
 930 *Science*, *264*(5161), 948–952. Retrieved from [https://science.sciencemag](https://science.sciencemag.org/content/264/5161/948)
 931 [.org/content/264/5161/948](https://science.sciencemag.org/content/264/5161/948) doi: 10.1126/science.264.5161.948